Journal of Biomedical Optics

BiomedicalOptics.SPIEDigitalLibrary.org

Structural modifications induced in dentin by femtosecond laser

Quang-Tri Le
Caroline Bertrand
Rui Vilar

SPIE.

Quang-Tri Le, Caroline Bertrand, Rui Vilar, "Structural modifications induced in dentin by femtosecond laser," *J. Biomed. Opt.* **21**(12), 125007 (2016), doi: 10.1117/1.JBO.21.12.125007.

Structural modifications induced in dentin by femtosecond laser

Quang-Tri Le,[a,b,*] Caroline Bertrand,[b] and Rui Vilar[a]
[a]Lisbon University, Instituto Superior Técnico and CeFEMA, Center of Physics and Engineering of Advanced Materials, Avenida Rovisco Pais, 1049-001 Lisboa, Portugal
[b]Laboratoire ICMCB, CNRS-UPR9048, 87 Avenue du Dr. Albert Schweitzer, 33608 Pessac Cedex, France

Abstract. The structural and chemical modifications induced in dentin by ultrafast laser ablation were studied. The laser experiments were performed with a Yb:KYW chirped-pulse-regenerative amplification laser system (560-fs pulse duration, 1030-nm radiation wavelength), fluences in the range 2 to 14 J/cm^2, 1-kHz pulse repetition rate, and 5-mm/s scanning speed. The ablation surfaces were characterized by scanning electron microscopy and Fourier transform infrared spectroscopy. The ablation surfaces produced with 2 J/cm^2 presented an irregular morphology with exposed dentinal tubules and no evidence of thermal effects. For 7 and 14 J/cm^2, the ablation surfaces were covered by a layer of redeposited ablation debris, consisting mainly of amorphous calcium phosphate. This layer is weakly adherent to the underlying tissue and can be easily removed by ultrasonication, revealing a surface with a morphology similar to the one obtained with 2 J/cm^2. The constitution of the dentin ablation surfaces is similar to the constitution of pristine dentin, showing that, within this fluence range, the laser treatment does not significantly modify the structure and constitution of dentin. The results achieved suggest an ablation mechanism where collagen is preferentially decomposed by the laser radiation, reducing the tissue cohesive strength and leading, ultimately, to its ablation. © *2016 Society of Photo-Optical Instrumentation Engineers (SPIE)* [DOI: 10.1117/1.JBO.21.12.125007]

Keywords: femtosecond laser; dentin; surface modification; ablation.

Paper 160686R received Oct. 3, 2016; accepted for publication Nov. 30, 2016; published online Dec. 21, 2016.

1 Introduction

Since their introduction to commercial use in the 1960s, lasers have been investigated as an alternative to mechanical drills for dental caries removal. The first investigations, based on CO_2 (wavelength ranging from 9.3 to 10.6 μm)[1–4] or Nd:YAG (wavelength 1064 nm)[5,6] lasers working in the CW regime or in the pulsed regime with pulse durations in the microsecond to millisecond range, showed that the laser treatment could be accompanied by undesirable thermal effects, such as melting, carbonization, thermomechanical cracking of dentin, and, in extreme cases, tooth pulp necrosis.[7] These phenomena are due to the thermal nature of the radiation–material interaction mechanisms for those lasers and their long interaction time, which lead to excessive heat transfer to the tooth. The use of Nd:YAG lasers with shorter pulse duration (in the 10^{-7} to 10^{-9} s range) allowed reducing thermal effects to some extent, but heating remained significant, leading to decomposition of hydroxyapatite, melting, denaturation of collagen, and thermomechanical cracking.[1,3,8,9] The accumulation of heat in the tooth during the laser treatment can be reduced by water cooling, but signs of melting are still observed, as reported by Fried et al.[10] for the ablation of enamel with a CO_2 laser with 8-μs pulse duration, 30-J/cm^2 fluence, and 300-Hz pulse repetition rate and by Zhang et al.[11] for the ablation of bone with a CO_2 laser with 100-μs pulse duration, 50-J/cm^2 fluence, and 50-Hz pulse repetition rate, the surface being covered by a water layer 1-mm thick.

Er,Cr:YSGG and Er:YAG lasers allow reducing the thermal degradation of dental tissues and, due to this advantage, became the main types of laser sources used in dentistry.[12,13] This is due to the particular ablation mechanism of dentin with these lasers. Their radiation wavelengths (2.78 and 2.94 μm, respectively) are within a strong absorption band of water.[14,15] Consequently, radiation is efficiently absorbed by the water contained in the tissue, which warms up and boils explosively, leading to the formation of a shockwave that disrupts the tissue.[16–18] This ablation mechanism reduces heat transfer to the tooth, but the shockwave created by the rapid water evaporation may lead to the formation of cracks.[19,20] Cracking can, however, be minimized by proper selection of the processing parameters.[21]

Thermal degradation of dental tissues can also be significantly reduced by using UV lasers.[22–26] Turkmen et al.[26] reported that the temperature increase in the tooth pulpal chamber during a laser treatment with an ArF excimer laser with 193-nm radiation wavelength and 15-ns pulse duration was significantly lower than the temperature increase produced during the same period of time with a 1064-nm radiation wavelength Nd:YAG laser with 150-μs pulse duration. This result was explained by Eugenio et al.[24] and Sivakumar et al.,[25] who showed that the ablation of intertubular dentin, which forms the bulk of the tooth, by a KrF excimer laser with 248-nm radiation wavelength and 30-ns pulse duration occurs predominantly by a photochemical mechanism, contrary to the photothermal ablation mechanism associated with CO_2 and Nd:YAG lasers,[16,27,28] leading to a significant reduction of thermal effects. However, despite their advantages, excimer lasers are not particularly suited for clinical use, because their ablation rate is low and the potential health hazard caused by exposure to intense UV radiation.

*Address all correspondence to: Quang-Tri Le, E-mail: quang.le@tecnico.ulisboa.pt

1083-3668/2016/$25.00 © 2016 SPIE

A more effective method to reduce thermal effects is by using ultrafast lasers. Femtosecond lasers allow ablating dentin efficiently and with negligible thermal degradation of the remaining tissue.[29–31] Alves et al.[30] showed that the surface of dentin specimens treated with fluences in the range 1 to 3 J/cm^2 were flat, with opened dentinal tubules, and showed no traces of melting or structural or compositional alterations of the underlying tissue. The ablation of enamel with a similar laser is accompanied by melting but the thickness of the molten layer is <1 μm and the tissue underneath remained unaltered.[32] This reduction of thermal effects is due to the fact that the pulse duration of these lasers is shorter than the electron-lattice energy transfer and the heat conduction characteristic times.[33] As a result, most of the energy absorbed by the electrons in the material is spent in the ablation process and carried away by the ablated material before significant heat transfer to the lattice may occur. However, ultrafast lasers can only be used clinically if material removal rates comparable to or higher than those obtained with conventional lasers are achieved and, for this to occur, high pulse repetition rates and high fluences must be used, increasing the risk of thermal damage. In this paper, the structural and compositional changes induced in dentin by ultrafast laser ablation with fluences up to 14 J/cm^2 at a pulse repetition rate of 1 kHz were investigated.

2 Materials and Methods

2.1 *Sample Preparation*

The experiments were performed using recently extracted human third molars. Tooth extraction was performed according to a protocol approved by the local Ethics Committee (process DC 2014/04) and with informed consent of the patients. Nineteen disks of dentin about 1.5-mm thick were cut parallel to the occlusal plane using a low-speed diamond saw (model Accutom-50, Struers, Denmark). The samples were stored in distilled water at 4°C. Less than 3 days before the laser experiments, one of the faces of these disks was polished under flowing water with a 600- to 2500-grit sequence of SiC abrasive papers. Prior to the laser treatment, the specimens were gently wiped with a clean paper tissue to remove the excess water.

The laser surface treatment was performed in ambient atmosphere using a Yb:KYW chirped-pulse-regenerative amplification laser system with a Gaussian beam, 560-fs pulse duration, 1030-nm radiation wavelength (model s-Pulse HP, Amplitude Systemes, France). The pulse repetition rate was 1 kHz. The laser beam was incident perpendicularly to the specimen surface and focused with a 100-mm focal length lens. In order to achieve the required radiation intensity, the specimen surface was located at a distance of 3 mm from the local plane, leading to a laser spot diameter, calculated by the D^2-method,[34] of ~71 μm. The pulse energy was varied with an attenuator to obtain average fluences in the range 2 to 14 J/cm^2. The average laser beam power, measured with a power meter (model 10ASHV1.1, Ophir Photonics, Israel), varied in the range 80 to 560 mW. The pulse energy, calculated from the average laser beam power and the pulse repetition rate, took values from 80 to 560 μJ. The specimens were moved under the stationary laser with a scanning velocity of 5 mm/s using a computer-controlled XY-stage (model LS-110, PI miCos, Germany).

In order to measure the ablation rate, linear tracks were created with fluences between 2 and 14 J/cm^2, 5-mm/s scanning speed, and 1-kHz pulse repetition rate. With these parameters, each surface spot receives 14 laser pulses, but the average fluence varies from pulse to pulse due to the Gaussian energy distribution in the laser beam. The ablation rate was calculated from the ablation volume using the following equation:

$$r_a = v * \frac{V_a}{f * L}, \tag{1}$$

where v is the scanning speed, f is the repetition rate, V_a is the ablated volume, and L is the length of the linear track. The ablation volume was calculated by integration of the three-dimensional surface profiles of the tracks, measured using a white light interferometer (model WYKO NT1100, Veeco). The values of the ablation rate presented are the average of three measurements performed in different regions of the tracks.

The morphology and the chemical constitution of the ablation surfaces were studied on specimens submitted to large area laser treatments with fluences of 2, 7, and 14 J/cm^2. These laser treatments were performed by overlapping individual tracks. Each track was created by moving the specimen in the X-direction at a velocity of 5 mm/s while pulsing the laser beam at 1 kHz. After completing the track, the specimen was returned to the origin of the movement, moved 0.01 mm in the Y-direction and another linear scan was performed in the X-direction. These steps were repeated until reaching complete surface coverage. With these parameters, overlap between consecutive tracks is 86% of the track width and each point of the surface received ~100 laser pulses, but the fluence varies from pulse to pulse due to the Gaussian energy distribution in the laser beam. Six specimens were tested for each value of the fluence. After the laser treatment, the specimens were rinsed in copious flowing water.

2.2 *Sample Characterization*

From the six dentin disks treated with each fluence, two were randomly chosen for the surface morphological analysis. Surfaces were observed by scanning electron microscopy (SEM), in the secondary electron imaging mode, with a field-emission gun scanning electron microscopy (JSM-7001F, JEOL, Japan) operated at an acceleration voltage of 10 kV. To avoid charging, the samples were coated with a conductive Pd/Au film prior to observation. The surfaces were observed in the laser-treated condition and after elimination of the ablation debris by ultrasonication. For cross-sectional SEM observation, the specimens were immersed in liquid N_2 and broken with a sharp hammer blow from the back side. The remaining specimens were analyzed by Fourier transform infrared (FTIR) spectroscopy in the attenuated total reflection mode with a Nicolet 5700 FTIR spectrometer (Thermo Electron Corporation) equipped with a solid-substrate beam splitter and a deuterated triglycine sulfate thermoelectrically cooled detector. The FTIR analysis was performed in the as-treated condition and after the elimination of the ablation debris layer by ultrasonication.

3 Results

3.1 *Ablation Rate*

The variation of average ablation rate with the radiation fluence is depicted in Fig. 1(a). The average ablation rate increases with fluence and reaches a value of 44×10^2 μm^3/pulse for 14 J/cm^2, corresponding to a material removal rate of

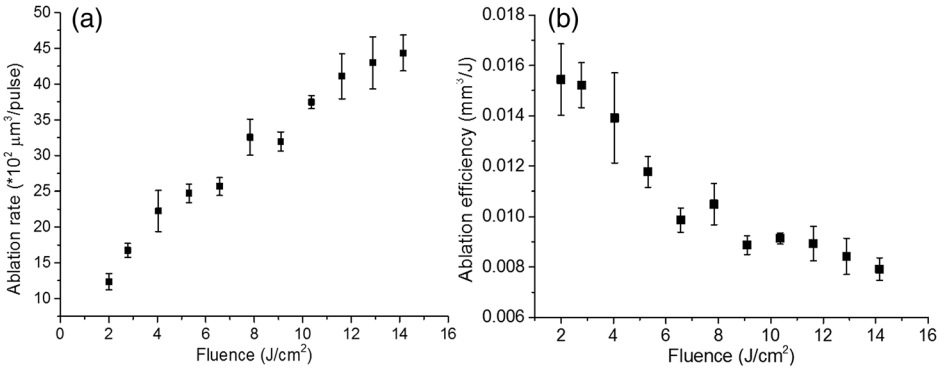

Fig. 1 (a) The evolution of the ablation rate and (b) ablation efficiency of dentin with radiation fluence.

0.44×10^{-2} mm^3/s. The evolution of the ablation efficiency, defined as the ablation volume per unit of laser pulse energy,[35] with the fluence is depicted in Fig. 1(b). The ablation efficiency reaches a maximum of 0.015 mm^3/J for 2 J/cm^2 and decreases with increasing fluence.

3.2 *Surface Morphology*

The surface morphology of specimens treated with 2, 7, and 14 J/cm^2 is depicted in the SEM micrographs of Fig. 2. The surface treated with 2 J/cm^2 is flat and presents an irregular morphology with open tubules and a very small amount of redeposited ablation debris [Fig. 2(a)]. The amount of ablation debris increases with fluence and the surfaces prepared with 7 and 14 J/cm^2 are covered by a continuous layer of ablation debris, aggregated in relatively large clusters [Figs. 2(c) and 2(e)]. The thickness of this layer and the size of the clusters increase with fluence. The layer of ablation debris is poorly adherent to the surface and can be removed by ultrasonication. The surface morphology after ultrasonication is presented in the micrographs of

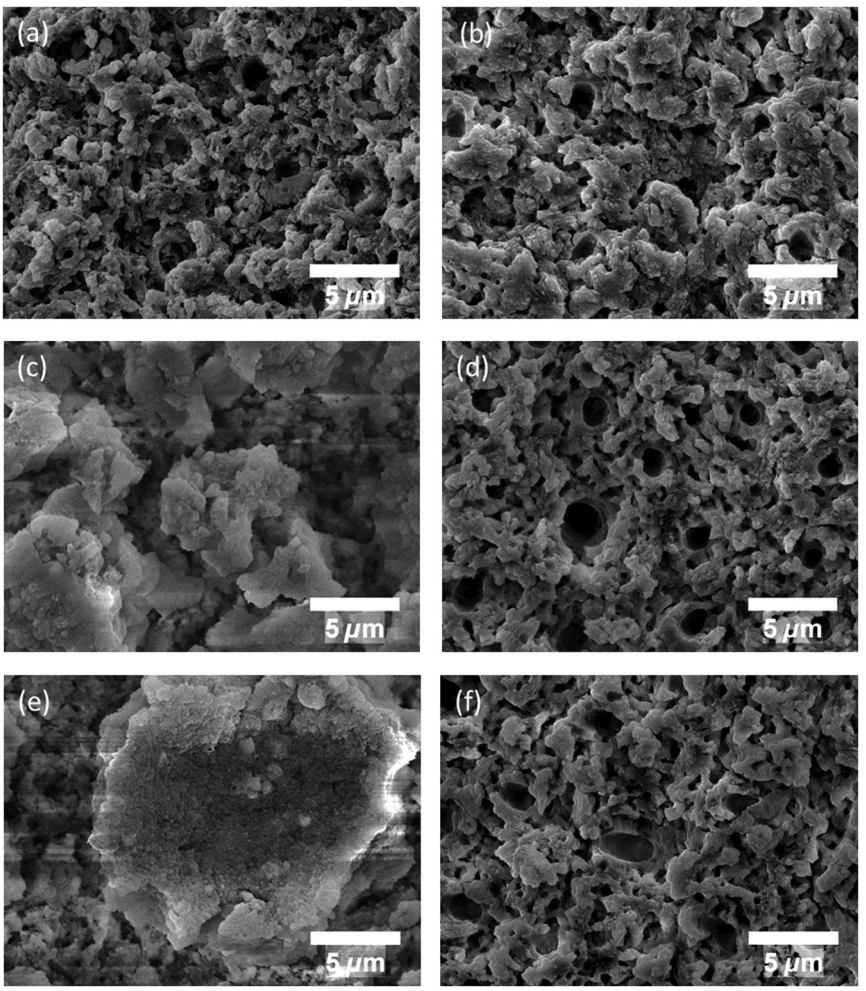

Fig. 2 Morphology of laser treated dentin surfaces before and after ultrasonication. Fluences (a) and (b) 2 J/cm^2, (c) and (d) 7 J/cm^2, and (e) and (f) 14 J/cm^2.

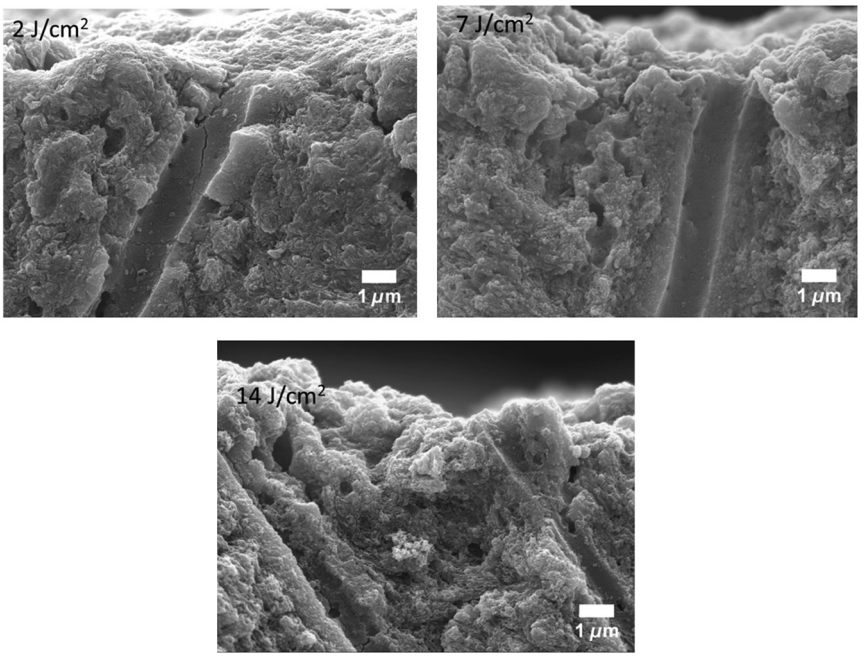

Fig. 3 Cross-sectional SEM images of laser treated specimens with 2, 7, and 14 J/cm^2.

Figs. 2(b), 2(d), and 2(f). The dentinal structure is now clearly exposed and the tubules are open. The observation of the transverse cross section of the laser treated specimens (Fig. 3) shows that no significant laser-induced damage occurred below the ablation surface and the tissue preserves its original morphology even in the specimens treated with a fluence of 14 J/cm^2.

3.3 *Surface Constitution*

The IR spectra of polished and laser-treated specimens, normalized to the largest amplitude peak, are shown in Fig. 4. This peak, located at 1005 cm^{-1}, corresponds to the ν_3 vibrational mode of the phosphate group of hydroxyapatite,[33,36] whereas the peak at 960 cm^{-1} can be assigned to the ν_1 vibrational mode of the same anion. The peak at 875 cm^{-1} corresponds to the ν_2 vibrational mode of the carbonate anion and the peaks at 1415 and 1450 cm^{-1} to the ν_3 vibrational mode of the same anion substituted in B-type PO_4^{3-} and A-type OH^-

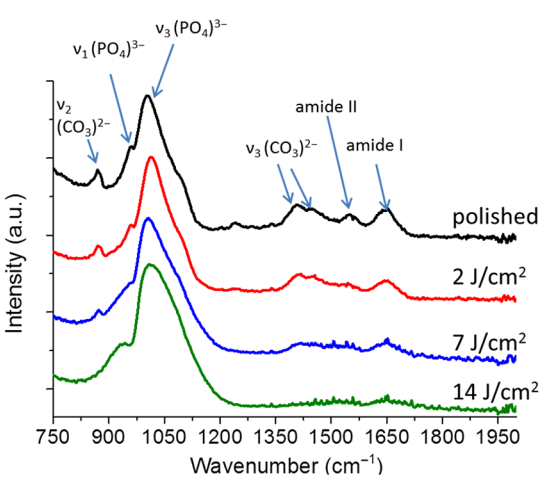

Fig. 4 Infrared spectra of polished and laser treated dentin specimens.

anionic sites, respectively.[33,36] The bands between 1680 and 1600 cm^{-1}, and 1580 and 1510 cm^{-1} correspond to the vibrational modes of amide I (C═O stretching) and amide II (C─N stretching and N─H deformation modes) groups of collagen, respectively.[33] The FTIR spectrum of the specimen treated with 2 J/cm^2 is similar to the spectrum of the polished specimen, showing that laser ablation with this low fluence does not significantly change the constitution of dentin. On the contrary, the spectra of the specimens treated with 7 and 14 J/cm^2 exhibit some differences as compared to untreated dentin. On the one hand, the amplitude of the peaks corresponding to vibrational modes of CO_3^{2-} and of the amides decreases after a laser treatment with 7 J/cm^2 and these peaks disappear when the surface treatment is performed with 14 J/cm^2. On the other hand, the width of the phosphate band at 1005 cm^{-1} increases and the well-defined phosphate peak at 960 cm^{-1}, which appears in the spectra of the polished specimen and of the specimens treated with 2 and 7 J/cm^2, is replaced by a broad band at 950 cm^{-1} in the spectrum of the specimen treated at 14 J/cm^2. Interestingly, the FTIR spectrum of the specimen treated with 14 J/cm^2 is similar to the spectrum of amorphous calcium phosphate (ACP),[37,38] indicating that this compound is the main constituent of the dentin surface after laser treatment with this fluence. ACP peaks are also observed in the spectra of the specimens treated with 7 J/cm^2, but their amplitudes are lower, indicating that the proportion of this compound in the surface layer decreased.

After removing the ablation debris with ultrasonication, the spectra of the specimens treated with 7 and 14 J/cm^2 become similar to the spectrum of the polished specimen (Fig. 5), indicating that the ACP exists mainly in the ablation debris and that the tissue underneath is unaffected by the ablation process. It should be emphasized that the depth of sampling of the FTIR spectroscopy method used, estimated assuming that the refractive index of dentin is 1.4 (Ref. 39) for the IR absorption spectral region of collagen (1650 cm^{-1}), is ~0.6 μm. Therefore, the thickness of the laser-induced damaged layer is <0.6 μm.

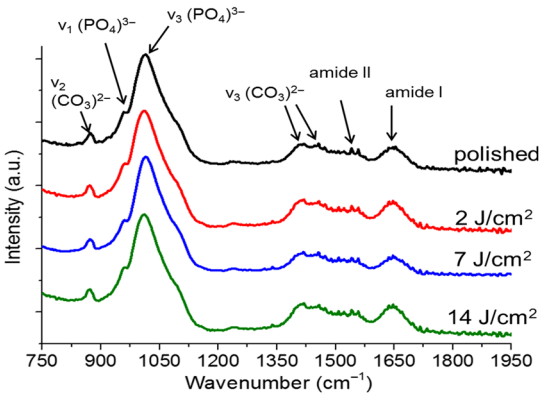

Fig. 5 Infrared spectra of laser treated specimens after ultrasonication.

4 Discussion

The results obtained in this work can be directly compared to those obtained by Alves et al.[30] with the same laser system and applying similar laser processing methods but lower fluences, in the range 1 to 3 J/cm^2. The surface morphology and constitution of the specimen treated with 2 J/cm^2 are in good agreement with the results of Alves et al.,[30] showing that the differences in behavior observed in this work for higher fluences are not due to sample variations, as may happen in biological tissues.[40] The main difference between the specimens treated with 2 J/cm^2 and those treated with higher fluences is the formation of a dense layer of ablation debris aggregated in clusters for the higher fluences. The size of the clusters and the thickness of the ablation debris layer increase with fluence. This evolution can be explained by the corresponding increase of the ablation rate (25×10^2 and 44×10^2 μm^3/pulse for 7 and 14 J/cm^2, respectively, as compared to 14 μm^3/pulse for 2 J/cm^2), which leads to an increase of the particles' collision probability in the plume and favors their coalescence into larger aggregates.[41] A similar variation of the cluster dimensions with fluence was observed by Trelenberg et al.[42] for GaAs. The FTIR analysis showed that the redeposited ablation debris consist mainly of ACP, the organic matter existing in dentin being decomposed at the high temperatures existing in the plume and in the redeposited debris. On the other hand, the extremely high cooling rates prevailing during the collapse of the plume explain why the calcium phosphate particles that redeposit on the surface present an amorphous structure.[37] After the removal of the ablation debris with ultrasonication, the underlying tissue morphology and constitution are similar, independent of the fluence used in the range of 2 to 14 J/cm^2. No traces of thermal degradation of the dental tissue are observed.

In a previous study,[32] the present authors showed that the ablation of human dental enamel in the same fluence range that was used in this work is accompanied by melting, leading to the formation of a continuous layer of resolidified calcium phosphate as well as by the projection of a large quantity of liquid droplets. These observation lead the authors to suggest that the predominant ablation mechanism of enamel in this fluence range is liquid spallation.[43,44] On the contrary, the ablation of dentin in the same fluence range is not accompanied by melting, even though the predominant phase in dentin and enamel is the same (hydroxyapatite). This difference in ablation behavior shows that the ablation mechanisms of dentin and enamel are different due to the different microstructures of both tissues. Dentin is a composite material consisting of hydroxyapatite nanocrystals dispersed in a network of collagen fibrils. Despite the fact that the predominant phase is hydroxyapatite (~70 wt.% in average), contrary to enamel, this phase is not continuous and the cohesive strength of dentin is ensured by the collagen fibrils.[45] These fibrils consist of long molecules where the atoms are bonded by covalent bonds, connected to one another by weak Van der Waals forces. As a result, collagen presents low thermal stability[46] and the ablation threshold for femtosecond laser radiation is also low (0.06 J/cm^2)[47] as compared to enamel, which consists entirely of hydroxyapatite (3.3 J/cm^2).[32] Collagen is degraded for relatively low radiation intensities, leading to a significant decrease of the strength of dentin and facilitating its ablation for radiation intensities lower than those required for hydroxyapatite-rich enamel and hydroxyapatite, which are ablated by liquid spallation or phase explosion depending on the laser processing parameters.[23,32,48] The present results support the ablation mechanism proposed by Alves et al.[30] for dentin. The authors observed that for fluences only slightly higher than the ablation threshold, the morphology of dentin surfaces treated with a femtosecond laser are very similar to brittle fracture surfaces and suggested that these surfaces should result from an ablation mechanism dominated by photomechanical fracture, with only very limited melting, a proposal that was supported by the results of the pump-probe experiments reported recently by Domke et al.[49] The authors observed extensive cracking around the ablation regions, but these cracks are due to dentin embrittlement by dehydration[50] and can be attenuated with water irrigation.[51] The contribution of solid spallation on the ablation of dentin was also demonstrated in this work by the angular shape of the ablation debris for the specimen treated with 2 J/cm^2. However, the proportion of resolidified droplets in the ablation debris increased with fluence, indicating that ablation mechanisms such as liquid spallation and phase explosion[43,44] play an increasingly important role in the ablation process as fluence increases, but these mechanisms are not the predominant dentin ablation mechanisms in the fluence range tested.

The results achieved in this work can be compared to those achieved with Er:YAG and Er, Cr:YSGG lasers. Ceballo et al.[13] observed a 3- to 5-μm-thick surface layer depleted in collagen followed by a 1-μm-thick layer where collagen was partially denatured in dentin surfaces treated with Er:YAG (23 J/cm^2 and 2 Hz) and similar observations were reported by Moretto et al.[20] for dentin treated with an Er, Cr:YSGG laser at 90 J/cm^2 and 20 Hz. The removal of collagen from these surfaces may explain the lower strength of the bonds between restorative adhesives and dentin surfaces prepared with Er:YAG and Er, Cr:YSGG lasers compared to surfaces prepared by mechanical methods,[13,52] because this bonding depends on the formation of a hybrid layer resulting from the impregnation of collagen by the adhesive,[53] which cannot occur if collagen is decomposed or denatured. This study shows that surface collagen is relatively well preserved when a femtosecond laser is used for the ablation of dentin. Moreover, after the removal of the ablation debris, a well-preserved dentin surface with open dentinal tubules, free of resolidified material and subsurface cracks exists. These characteristics are all favorable for the formation of a strong bond between dentin and dental restorative adhesives.

The maximum ablation efficiency achieved in this work was 0.015 mm^3/J for 2 J/cm^2, similar to the value obtained for a laser with 1025-nm radiation wavelength and 400-fs pulse

duration at a fluence of 4.69 J/cm^2 (0.018 mm^3/J)[54] and lower than the value achieved for an Er:YAG laser (0.025 mm^3/J for 203.7 J/cm^2).[55] The ablation efficiency decreases with increasing fluence for fluences higher than 2.8 J/cm^2, in contradiction with the trend observed by Chen et al.[56] (an increase of the ablation efficiency with fluence in the range 1 to 6 J/cm^2 followed by a decrease between 6 and 11 J/cm^2). This difference in behavior can be explained by the different average number of pulses per surface spot used in the two works (14 and 1.6, respectively). Neuenschwander et al.[57] showed that the ablation efficiency depends on the ratio F/F_{th}, where F is the radiation fluence and F_{th} is the material ablation threshold. The ablation threshold of hard tissues such as enamel,[58] cortical bone,[33] and dentin[59] decreases with increasing number of laser pulses, a dependence that was explained by Jee et al.[60] assuming that laser irradiation of materials at fluences lower than the ablation threshold create defects in the material that lead to an increase of its absorption coefficient. The corresponding effect on the ablation threshold can be expressed by

$$F_{th}(N) = F_{th}(1) * N^{S-1}, \quad (2)$$

where F_{th} (1) and F_{th} (N) and S are the ablation thresholds for a single pulse and for N pulses and the incubation coefficient, respectively. Assuming that the incubation coefficient of dentin is similar to the incubation factor of cortical bone (0.8) and that its single-pulse ablation threshold is 0.6 J/cm^2,[30] the average ablation threshold values for 14 in this work, and 1.6, in the work by Chen et al.,[54] laser pulses, calculated by Eq. (2), are 0.35 and 0.55 J/cm^2, respectively. If expressed in terms of F/F_{th} as suggested by Neuenschwander et al.[57] instead of F, in the fluence range used by Chen et al.[54] ($2.75 < F/F_{th} < 14.30$) the ablation efficiency increases first, passes through a maximum for $F/F_{th} \sim 8.58$, then decreases. In the fluence range used in this work ($5.65 < F/F_{th} < 39.56$), the decrease of the ablation efficiency with fluence can be clearly observed for $F/F_{th} > 7.9$ ($F > 2.8$ J/cm^2), showing good agreement between the two works.

The maximum material removal rate found in this work (0.44×10^{-2} mm^3/s for 14 J/cm^2) is significantly lower than the removal rate obtained with mechanical drilling (~1 mm^3/s).[35] This value shows that femtosecond lasers can only be applied for carious dentin removal with higher fluences and higher repetition rates to achieve high caries removal rates.

5 Conclusion

This study shows that the structure and constitution of dentin are preserved when the tissue is ablated using 560-fs laser pulses of 1030-nm radiation, fluences in the range 2 to 14 J/cm^2, and 1-kHz repetition rate. The ablation surface obtained with a fluence of 2 J/cm^2 shows a scaly appearance and is free of melting, carbonization, or cracking. For higher fluences, a loosely attached layer of redeposited ablation debris covers the ablation surfaces, but this layer can be easily removed with ultrasonication, revealing a surface morphology similar to the one found for 2 J/cm^2. The ablation debris consists mainly of ACP. The absence of surface melting, the morphology of the dentin ablation surfaces, and the shape of the ablation debris suggest that the ablation on dentin in the fluence range used in this work occurs predominantly by a photomechanical mechanism (solid spallation) instead of the photothermal mechanisms reported for enamel and hydroxyapatite.

Disclosures

The authors confirm that there are no conflicts of interest.

Acknowledgments

Q. T. Le gratefully acknowledges a PhD grant of the Erasmus Mundus Program International Doctoral School of Functional Materials (IDS FunMat) Project No. 2013-14. This work was financially supported by the ERASMUS MUNDUS Agency EACEA (Contract No. 2010-0004/0001) via the program International Doctoral School of Functional Materials (IDS FunMat). The protocol for teeth collection used in this work was approved by local Ethic Committee (process DC 2014/04). Informed consents from the patients were obtained before the collection.

References

1. V. B. Krapchev, C. D. Rabii, and J. A. Harrington, "Novel CO_2 laser system for hard tissue ablation," *Proc. SPIE* **2128**, 341–348 (1994).
2. D. Fried et al., "Multiple pulse irradiation of dental hard tissues at CO_2 laser wavelengths," in *Proc. Lasers Dentistry*, Vol. 2394, pp. 41–50 (1995).
3. M. Staninec et al., "Pulpal effects of enamel ablation with a microsecond pulsed lambda = 9.3-microm CO_2 laser," *Lasers Surg. Med.* **41**, 256–263 (2009).
4. I. W. M. Jeffrey et al., "Dentinal temperature transients caused by exposure to CO2 laser irradiation and possible pulpal damage," *J. Dent.* **18**, 31–36 (1990).
5. D. M. Harris et al., "Selective ablation of surface enamel caries with a pulsed Nd:YAG dental laser," *Lasers Surg. Med.* **30**, 342–350 (2002).
6. V. Armengol, A. Jean, and D. Marion, "Temperature rise during Er: YAG and Nd: YAP laser ablation of dentin," *J. Endod.* **26**, 138–141 (2000).
7. Y. Launay et al., "Thermal effects of lasers on dental tissues," *Lasers Surg. Med.* **7**, 473–477 (1987).
8. A. McDonald et al., "The effect of Nd: YAG radiation at nanosecond pulse duration on dentine crater depth," *Biomaterials* **23**, 51–58 (2002).
9. S. Kuroda and B. O. Fowler, "Compositional, structural, and phase changes in in vitro laser-irradiated human tooth enamel," *Calcif. Tissue Int.* **36**, 361–369 (1984).
10. D. Fried et al., "Dissolution studies of bovine dental enamel surfaces modified by high-speed scanning ablation with a lambda = 9.3-microm TEA CO(2) laser," *Lasers Surg. Med.* **38**, 837–845 (2006).
11. X. Zhang et al., "Influence of water layer thickness on hard tissue ablation with pulsed CO_2 laser," *J. Biomed. Opt.* **17**, 038003 (2012).
12. S. R. Visuri, J. T. Walsh, and H. A. Wigdor, "Erbium laser ablation of dental hard tissue: effect of water cooling," *Lasers Surg. Med.* **18**, 294–300 (1996).
13. L. Ceballo et al., "Bonding to Er-YAG-laser-treated dentin," *J. Dent. Res.* **81**, 119–122 (2002).
14. L. Bachmann et al., "Changes in chemical composition and collagen structure of dentine tissue after erbium laser irradiation," *Spectrochim. Acta Part A Mol. Biomol. Spectrosc.* **61**, 2634–2639 (2005).
15. Y. Nishimoto et al., "Effect of pulse duration of Er:YAG laser on dentin ablation," *Dent. Mater. J.* **27**, 433–439 (2008).
16. D. Fried, J. Ragadio, and A. Champion, "Residual heat deposition in dental enamel during IR laser ablation at 2.79, 2.94, 9.6, and 10.6 microm," *Lasers Surg. Med.* **29**, 221–229 (2001).
17. L. Bachmann et al., "Crystalline structure of human enamel irradiated with Er, Cr:YSGG laser," *Laser Phys. Lett.* **6**, 159–162 (2009).
18. M. Mir et al., "Influence of water-layer thickness on Er:YAG laser ablation of enamel of bovine anterior teeth," *Lasers Med. Sci.* **23**, 451–457 (2008).
19. L. E. Rodriguez-Vilchis et al., "Morphological and structural changes on human dental enamel after Er:YAG laser irradiation: AFM, SEM, and EDS evaluation," *Photomed. Laser Surg.* **29**, 493–500 (2011).
20. S. G. Moretto et al., "Effects of ultramorphological changes on adhesion to lased dentin-scanning electron microscopy and transmission electron microscopy analysis," *Microsc. Res Tech.* **74**, 720–726 (2011).

21. B. S. Lee, Y. L. Hung, and W. H. Lan, "Compositional and morphological changes of human dentin after Er:YAG laser irradiation," *Int. Congr. Ser.* **1248**, 143–152 (2003).
22. F. Sanchez, A. J. Espana Tost, and J. L. Morenza, "ArF excimer laser irradiation of human dentin," *Lasers Surg. Med.* **21**, 474–479 (1997).
23. S. Eugénio et al., "KrF laser treatment of human dentin," *Proc. SPIE* **7131**, 71311M (2008).
24. S. Eugenio et al., "Characterisation of dentin surfaces processed with KrF excimer laser radiation," *Biomaterials* **26**, 6780–6787 (2005).
25. M. Sivakumar et al., "Influence of tubule orientation on cone-shaped texture development in laser-ablated dentin," *Lasers Med. Sci.* **21**, 160–164 (2006).
26. C. Turkmen et al., "Effect of CO2, Nd:YAG, and ArF excimer lasers on dentin morphology and pulp chamber temperature: an in vitro study," *J. Endod.* **26**, 644–648 (2000).
27. D. Fried et al., "Thermal and chemical modification of dentin by 9-11-μm CO_2 laser pulses of 5-100-μs duration," *Lasers Surg. Med.* **31**, 275–282 (2002).
28. A. Antunes, W. de Rossi, and D. M. Zezell, "Spectroscopic alterations on enamel and dentin after nanosecond Nd: YAG laser irradiation," *Spectrochim. Acta Part A* **64**, 1142–1146 (2006).
29. J. Neev et al., "Ultrashort pulse lasers for hard tissue ablation," *IEEE J. Sel. Top. Quantum Electron.* **2**, 790–800 (1996).
30. S. Alves, V. Oliveira, and R. Vilar, "Femtosecond laser ablation of dentin," *J. Phys. D Appl. Phys.* **45**, 245401 (2012).
31. A. V. Rode et al., "Precision ablation of dental enamel using a subpicosecond pulsed laser," *Aust. Dent. J.* **48**, 233–239 (2003).
32. Q. T. Le and R. V. C. Bertrand, "Femtosecond laser ablation enamel," *J. Biomed. Opt.* **21**, 065005, (2016).
33. L. T. Cangueiro et al., "Femtosecond laser ablation of bovine cortical bone," *J. Biomed. Opt.* **17**, 125005 (2012).
34. J. M. Liu, "Simple technique for measurements of pulsed Gaussian-beam spot sizes," *Opt. Lett.* **7**, 196–198 (1982).
35. M. S. Bello-Silva et al., "Precise ablation of dental hard tissues with ultra-short pulsed lasers. Preliminary exploratory investigation on adequate laser parameters," *Lasers Med. Sci.* **28**, 171–184 (2013).
36. I. Rehman and W. Bonfield, "Characterization of hydroxyapatite and carbonated apatite by photo acoustic FTIR spectroscopy," *J. Mater. Sci. Mater. Med.* **8**, 1–4 (1997).
37. C. Combes and C. Rey, "Amorphous calcium phosphates: synthesis, properties and uses in biomaterials," *Acta Biomater.* **6**, 3362–3378 (2010).
38. D. Skrtic, J. M. Antonucci, and E. D. Eanes, "Amorphous calcium phosphate-based bioactive polymeric composites for mineralized tissue regeneration," *J. Res. Natl. Inst. Stand. Technol.* **108**, 167–182 (2003).
39. J. Laffitte and D. Roelant, *Experimental Characterization of Near Infrared Laser Energy Absorption Scattering and Transmittance in Biological Tissue*, Air Force Research Laboratory, USA (2007).
40. M. Anwar Alebrahim et al., "ATR-FTIR and Raman spectroscopy of primary and permanent teeth," *Biomed. Spectrosc. Imaging* **3**, 15–27 (2014).
41. T. E. Itina et al., "Mechanisms of small clusters production by short and ultra-short laser ablation," *Appl. Surf. Sci.* **253**, 7656–7661 (2007).
42. T. W. Trelenberg et al., "Femtosecond pulsed laser ablation of GaAs," *Appl. Surf. Sci.* **221**, 364–369 (2004).
43. L. V. Zhigilei, Z. Lin, and D. S. Ivanov, "Atomistic modeling of short pulse laser ablation of metals: connections between melting, spallation, and phase explosion," *J. Phys. Chem. C* **113**, 11892–11906 (2009).
44. D. Perez and L. J. Lewis, "Molecular-dynamics study of ablation of solids under femtosecond laser pulses," *Phys. Rev. B* **67**, 184102 (2003).
45. V. Imbeni et al., "The dentin-enamel junction and the fracture of human teeth," *Nat. Mater.* **4**, 229–232 (2005).
46. S. R. Armstrong et al., "Denaturation temperatures of dentin matrices. I. Effect of demineralization and dehydration," *J. Endod.* **32**, 638–641 (2006).
47. A. A. Oraevsky et al., "Plasma mediated ablation of biological tissues with nanosecond-to-femtosecond laser pulses: relative role of linear and nonlinear absorption," *IEEE J. Sel. Top. Quantum Electron.* **2**, 801–809 (1996).
48. J. Kruger, W. Kautek, and H. Newesely, "Femtosecond-pulse laser ablation of dental hydroxyapatite and single-crystalline fluoroapatite," *Appl. Phys. A* **69**, S403–S407 (1999).
49. M. Domke et al., "Investigations of the damage mechanisms during ultrashort pulse laser ablation of dental tissue," *Proc. SPIE* **9542**, 95420Q (2015).
50. J. J. Kruzic et al., "Crack blunting, crack bridging and resistance-curve fracture mechanics in dentin: effect of hydration," *Biomaterials* **24**, 5209–5221 (2003).
51. L. T. Cangueiro and R. Vilar, "Influence of the pulse frequency and water cooling on the femtosecond laser ablation of bovine cortical bone," *Appl. Surf. Sci.* **283**, 1012–1017 (2013).
52. W. J. Dunn, J. T. Davis, and A. C. Bush, "Shear bond strength and SEM evaluation of composite bonded to Er:YAG laser-prepared dentin and enamel," *Dent. Mater.* **21**, 616–624 (2005).
53. B. Van Meerbeek et al., "Buonocore memorial lecture. Adhesion to enamel and dentin: current status and future challenges," *Oper. Dent.* **28**, 215–235 (2003).
54. H. Chen et al., "Femtosecond laser for cavity preparation in enamel and dentin: ablation efficiency related factors," *Sci. Rep.* **6**, 20950 (2016).
55. J. Meister et al., "Influence of the water content in dental enamel and dentin on ablation with erbium YAG and erbium YSGG lasers," *J. Biomed. Opt.* **11**, 034030 (2006).
56. H. Chen et al., "Femtosecond laser ablation of dentin and enamel: relationship between laser fluence and ablation efficiency," *J. Biomed. Opt.* **20**, 028004 (2015).
57. B. Neuenschwander et al., "Surface structuring with ultra-short laser pulses: basics, limitations and needs for high throughput," *Phys. Proc.* **56**, 1047–1058 (2014).
58. Q.-T. Le, C. Bertrand, and R. Vilar, "Femtosecond laser ablation of enamel," *J. Biomed. Opt.* **21**, 065005 (2016).
59. G. Nicolodelli, F. R. de Lizarelli, and V. S. Bagnato, "Influence of effective number of pulses on the morphological structure of teeth and bovine femur after femtosecond laser ablation," *J. Biomed. Opt.* **17**, 048001 (2012).
60. Y. Jee, M. F. Becker, and R. M. Walser, "Laser-induced damage on single-crystal metal surfaces," *J. Opt. Soc. Am. B* **5**, 648–659 (1988).

Biographies for the authors are not available.